

$A/B$  that can be deduced from Fig. 3. By substituting  $S$  and  $T_{2e} = 9 \times 10^{-8}$  sec in Eq. (21) we have, however,

$$B/C \approx \frac{1}{4} T_{2e}^2 S^2 \approx 250 \rightarrow 24 \text{ dB} ,$$

which is greater than the value that can be read from Fig. 3; however, because the harmonic signal at  $\omega = \omega_0$  has the same intensity as the noise, the true ratio  $B/C$  in Fig. 3 can be much greater than 13 dB. On the other hand, by substituting in the equation  $S = \gamma H_x (T_1/T_2)^{1/2}$  the proper values of  $H_x$ ,  $T_1$ , and  $T_2$ , we obtain for  $S$ , values very close to those obtained from linewidth measurements of the  $\omega \sim \omega_0$  line.

Finally, we remark that all of the previous data

are taken with the magnetic field geometry of Fig. 2. By using a different magnetic field geometry, we can split the second-harmonic emission signal into a contribution that is due to  $M_x(2\omega)$  and one that is due to  $M_z(2\omega)$ . In particular, if we operate with  $\vec{H}_{rf}(\omega)$  perpendicular to  $\vec{H}_0$  and  $\vec{H}_{rf}(2\omega)$  parallel to  $\vec{H}_0$ , only the component  $M_x(2\omega)$  is different from zero, and, therefore, one single line, near  $\omega = \omega_0$ , is expected. Actually, by using a cavity with this magnetic field geometry, the detected harmonic spectrum shows only the  $\omega \sim \omega_0$  line.

#### ACKNOWLEDGMENTS

We acknowledge very useful conversations with G. Vetri and F. S. Persico.

\*On sabbatical leave from the Department of Physics and Research Laboratory of Electronics, Massachusetts Institute of Technology, Cambridge, Mass. 02139.

<sup>1</sup>R. Karplus and J. Schwinger, Phys. Rev. **73**, 1020 (1948); M. A. Garstens and J. I. Kaplan, *ibid.* **99**, 459 (1955).

<sup>2</sup>R. Karplus, Phys. Rev. **73**, 1027 (1948).

<sup>3</sup>R. Boscaino, I. Ciccarello, and C. Cusumano, Phys. Rev. Letters **20**, 421 (1968).

<sup>4</sup>N. Bloembergen and Y. R. Shen, Phys. Rev. **133**, A37 (1964); N. Bloembergen, *Nonlinear Optics* (Benjamin, New York, 1965).

<sup>5</sup>J. Brossel, B. Cagnac, and A. Kastler, Compt. Rend. **237**, 984 (1953).

<sup>6</sup>J. M. Winter, J. Phys. Radium **19**, 802 (1958).

<sup>7</sup>G. Alzetta, E. Arimondo, C. Ascoli, and A. Gozzini, Nuovo Cimento **52B**, 392 (1967).

<sup>8</sup>G. Alzetta, E. Arimondo, and C. Ascoli, Nuovo Cimento **54B**, 107 (1968).

<sup>9</sup>J. M. Winter, Ann. Phys. (Paris) **4**, 745 (1959).

<sup>10</sup>F. Lurcat, Arch. Sci. (Geneva) **11**, 295 (1958).

<sup>11</sup>S. Wilking, Z. Physik, **173**, 490 (1963).

<sup>12</sup>A. G. Redfield, Phys. Rev. **98**, 1787 (1955).

<sup>13</sup>B. N. Provotorov, Zh. Eksperim. i Teor. Fiz. **41**, 1582 (1961) [Soviet Phys. JETP **14**, 1126 (1962)]; G. R. Khutsishvili, *ibid.* **50**, 1641 (1966) [*ibid.* **23**, 1092 (1966)].

<sup>14</sup>F. S. Persico and G. Vetri, Solid State Commun. **8**, 1509 (1970).

<sup>15</sup>J. P. Goldsborough, N. Mandel, and G. E. Pake, Phys. Rev. Letters **4**, 13 (1960).

<sup>16</sup>W. J. C. Grant and M. W. P. Strandberg, Phys. Rev. **135**, A727 (1964).

<sup>17</sup>R. Boscaino, I. Ciccarello, and M. W. P. Strandberg (unpublished).

## Scattering from the $E_1$ Polariton of $\text{LiIO}_3$

C. K. Asawa and M. K. Barnoski

*Hughes Research Laboratories, Malibu, California 90265*

(Received 16 November 1970)

Raman scattering from an  $E_1$  mode polariton of  $\text{LiIO}_3$  is reported. A polariton with energy between 687 and 766  $\text{cm}^{-1}$  is observed in near-forward scattering with  $y(xz)\bar{y}$  polarization. The polariton is observed only near 764  $\text{cm}^{-1}$  in the  $y(xz)\bar{y}$  spectra. The results are analyzed. It is also found that the polariton dispersion curve does not change with the orientation of the phonon wave vector.

### INTRODUCTION

It was shown by Huang<sup>1</sup> that transverse optical phonons of ionic crystals and photons with nearly the same wave vector and energy can be strongly coupled. The resulting mixed phonon-photon states are now referred to as "polaritons." Raman scattering from the polaritons of GaP was reported for the first time by Henry and Hopfield.<sup>2</sup> Shortly thereafter polariton scattering from anisotropic ZnO

was reported by Porto *et al.*<sup>3</sup>

The Raman and polariton spectra of  $\text{LiIO}_3$  have been examined recently by Claus *et al.*<sup>4</sup> These authors stated that no  $E_1$  polariton was "unambiguously" observed [although an A polariton was observed in  $x(yy)x$  polarization]. We wish to report the observation of an  $E_1$  polariton in forward scattering in  $\text{LiIO}_3$  and to clarify possible difficulties in the analysis of the experiments.

$\text{LiIO}_3$  belongs to the  $P6_3(C_2)$  space group.<sup>5</sup> Twen-

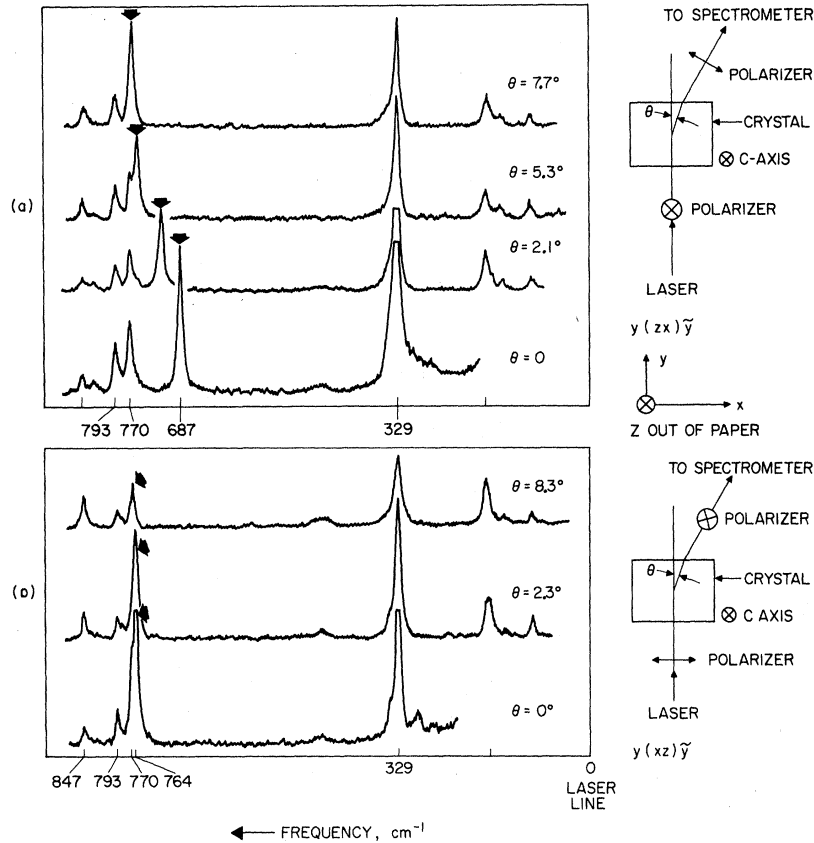


FIG. 1. Near-forward-scattering spectra for the  $E_1$  mode of  $\text{LiIO}_3$ . The arrows point to the polariton line discussed in this paper. (a)  $y(zx)y$  polarization, where  $\hat{y}$  lies in the  $xy$  plane.  $\theta$  is the forward-scattering angle, i.e., the small angle between the incident and scattered photon propagation directions. (b)  $y(xz)y$  polarization; asymmetry of the two spectra is discussed in the text.

ty-seven optical-phonon modes are allowed:  $4A + 5B + 4E_1 + 5E_2$ . The  $A(z)$ ,  $E_1(x)$ , and  $E_2(y)$  modes are both infrared and Raman active, permitting possible observation of polariton modes.

### RESULTS AND DISCUSSION

The  $y(zx)y$  and  $y(xz)y$  forward-scattering spectra<sup>6</sup> are shown in Fig. 1. Figure 1(a) shows the polariton line for the  $y(zx)y$  polarization for various forward-scattering angles, starting at  $687\text{ cm}^{-1}$  at  $\theta = 0^\circ$ . The polariton line appears to approach and coalesce with the  $770\text{-cm}^{-1}$  line as the scattering angle  $\theta$  is increased. The  $5145\text{-\AA}$  argon laser line was used.

An intense line at  $764\text{ cm}^{-1}$ , with a slight shoulder at  $770\text{ cm}^{-1}$ , was observed in the  $y(xz)y$  spectra for  $0^\circ$  scattering. This is shown in Fig. 1(b). With increasing forward-scattering angles, the  $764\text{-cm}^{-1}$  line decreased in intensity relative to the  $770\text{-cm}^{-1}$  line.

The apparent asymmetry in the polarizability components  $\alpha_{xx}$  and  $\alpha_{zz}$  observed in Figs. 1(a) and 1(b) for the polariton is a result of the difference in refractive indices associated with the two different scattering geometries.

Employing the momentum- and energy-conservation laws and using the small-angle approximation (see Fig. 2), the dispersion relationship for polaritons is easily shown to be

$$k^2 = (1/c^2) \{ [(n_i - n_s)\omega_i + n_s\omega]^2 + n_i n_s \omega_i (\omega_i - \omega) \theta^2 \},$$

where  $n_i$  and  $n_s$  are the refractive indices for the incident and scattered photons, respectively, and  $\theta$  is the scattering angle. The results obtained for the frequency vs wave vector of the polariton is shown in Fig. 3. The open circles were calculated using the  $y(zx)y$  scattering geometry. In this case,  $n_i = n_e$  (extraordinary wave) and  $n_s = n_o$  (ordinary wave). The corresponding scattering angles are shown with the computed points. The open squares were obtained from the  $y(xz)y$  scattering geometry. For this configuration,  $n_i = n_o$  and  $n_s = n_e$ . It is noted that each forward-scattering angle corresponds to two different points on the single dispersion curve for the two different scattering geometries. The results shown in Fig. 3 describe the spectra shown in Figs. 1(a) and 1(b).

The phonon directions for the above cases lie in the  $xy$  plane since the incident and scattered photons both lie in the plane. Therefore, only the magnitude, not the direction, of the polariton wave vector determine the dispersion curve.

However, if the polariton wave vector lies in the  $yz$  plane, mixing of the  $E_1$  and  $A$  modes may be expected.<sup>7</sup> Therefore, a number of forward-scattering spectra with the  $y(zx)y$  geometry were taken, where  $\hat{y}$ , and therefore  $\vec{k}$ , lies in the  $yz$  plane. The

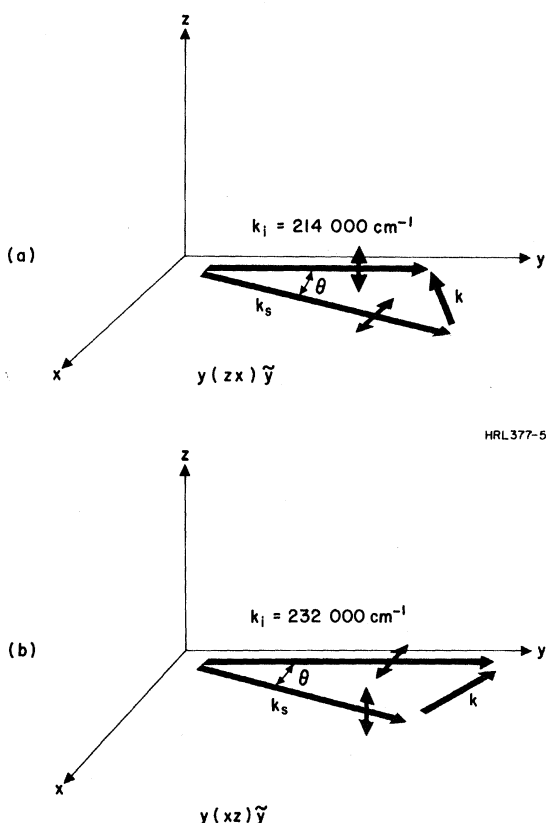


FIG. 2. Momentum-conservation triangles for the two scattering geometries used. (a)  $y(zx)\tilde{y}$  polarization with  $n_i = n_o$ ,  $n_s = n_o$ , and  $k_i < k_s$ . The range of polariton wave vector is  $10\,000\text{ cm}^{-1}$  (at  $\theta = 0^\circ$ )  $\leq k_{\text{polariton}} \leq 31\,000\text{ cm}^{-1}$  (at  $\theta = 7.7^\circ$ ). (b)  $y(xz)\tilde{y}$  polarization with  $n_i = n_o$ ,  $n_s = n_o$ , and  $k_i > k_s$ . The range of polariton wave vector is  $26\,000\text{ cm}^{-1}$  (at  $\theta = 0^\circ$ )  $\leq k_{\text{polariton}} \leq 36\,000\text{ cm}^{-1}$  (at  $\theta = 5.7^\circ$ ), and  $n_o = 1.90$ ,  $n_o = 1.75$ .

spectra obtained were compared with the  $y(xz)\tilde{y}$  spectra for equal scattering angles. No difference in the polariton frequencies for the two different geometries was observed for scattering angles  $\theta$  between  $0^\circ$  and  $7.7^\circ$ . For the  $y(zx)\tilde{y}$  case, the angle between the phonon vector  $\vec{k}$  and the  $xy$  plane varied from  $0$  to  $76^\circ$  as  $\theta$  varied from  $0$  to  $7.7^\circ$ . This result suggests that the strong coupling between radiation field and lattice vibration, which gives rise to the  $E_1$  polariton mode described here, dominates the lattice anisotropy which mixes the  $A$  and  $E_1$  lattice waves.

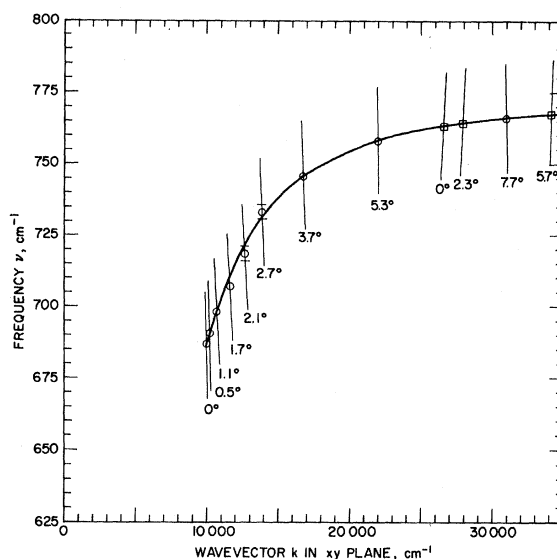


FIG. 3.  $E_1$ -mode polariton dispersion curve near  $k=0$  for  $\text{LiIO}_3$  as determined from near-forward scattering of  $y(zx)\tilde{y}$  and  $y(xz)\tilde{y}$  polarizations. Points denoted by the open circles were computed from the experimental data for the various forward-scattering angles  $\theta$ , as indicated, for the  $y(zx)\tilde{y}$  polarization. Points denoted by the open squares are those for the  $y(xz)\tilde{y}$  polarization.

### SUMMARY

Even though the  $E_1$  polariton spectra of  $\text{LiIO}_3$  shown in Figs. 1(a) and 1(b) appears to be markedly asymmetric, the above analysis shows that this can be accounted for by a single polariton dispersion curve. In many uniaxial and biaxial crystals the indices and frequency differences can be such that a large asymmetry in the polariton spectra can result. This cannot be interpreted as an asymmetry in the polarizability tensor.

In addition, it was found that the  $E_1$  polariton dispersion curve does not change with the orientation of the phonon wave vector for small scattering angles.

### ACKNOWLEDGMENTS

We are greatly indebted to A. C. Pastor and R. C. Pastor for growing and providing us with several large lithium iodate crystals. We wish to thank D. Tseng for lending us a cut sample.

<sup>1</sup>K. Huang, Proc. Roy. Soc. (London) **A208**, 352 (1951).

<sup>2</sup>C. H. Henry and J. J. Hopfield, Phys. Rev. Letters **15**, 964 (1965).

<sup>3</sup>S. P. S. Porto, B. Tell, and T. C. Damen, Phys. Rev. Letters **16**, 450 (1966).

<sup>4</sup>R. Claus, H. W. Schrotter, H. H. Hacker, and

S. Haussuhl, Z. Naturforsch. **24a**, 1733 (1969).

<sup>5</sup>A. Rosenzweig and R. Morosin, Acta. Cryst. **20**, 758 (1966).

<sup>6</sup> $\tilde{y}$  denotes that the scattered photon is in the  $xy$  plane.

<sup>7</sup>W. Otaguro, C. A. Arguello, and S. P. S. Porto, Phys. Rev. B **1**, 2818 (1970).